

High-pressure study of the β -to- α transition in Ga_2O_3

Denis Machon,¹ Paul F. McMillan,^{1,2,*} Bin Xu,³ and Jianjun Dong³

¹*Department of Chemistry and Materials Chemistry Centre, Christopher Ingold Laboratories, University College London, 20 Gordon Street, London WC1H 0AJ, United Kingdom*

²*Davy-Faraday Research Laboratory, Royal Institution of Great Britain, 21 Albemarle Street, London W1X 4BS, United Kingdom*

³*Physics Department, Auburn University, Auburn, Alabama 36849, USA*

(Received 7 January 2006; published 28 March 2006)

The high-pressure behavior of Ga_2O_3 is studied up to 40 GPa using synchrotron x-ray diffraction and Raman spectroscopy in diamond anvil cells. A phase transformation from the monoclinic β -phase ($C2/m$) is observed at a pressure above 20–22 GPa. The high-pressure polymorph is identified as the α -phase that is isostructural with corundum ($R\bar{3}c$ symmetry) from the x-ray diffraction data. However, considerable anion disorder is indicated by the appearance of broad bands in the Raman spectra. The experimental results are complemented by *ab initio* theoretical calculations of the energetics of the two structures and the lattice dynamics.

DOI: [10.1103/PhysRevB.73.094125](https://doi.org/10.1103/PhysRevB.73.094125)

PACS number(s): 64.70.Kb, 62.50.+p, 63.20.Dj

I. INTRODUCTION

The oxides of group 13 elements (Al, Ga, In) are important solid-state compounds with applications in fields ranging from structural ceramics to catalysts and electronic materials.¹ Monoclinic gallium oxide (Ga_2O_3) is usually known as a wide-band-gap semiconductor ($E_g=4.9$ eV); however, the conductivity can be varied from insulating to conducting behavior depending upon the preparation conditions.² Due to its tunable optical and electronic properties, β - Ga_2O_3 is being developed for use in a wide variety of applications, for instance, as optical windows,³ in high-temperature chemical gas sensors,⁴ as a magnetic memory material,⁵ and for dielectric thin films.⁶ Recently, considerable effort has been devoted to the study of low-dimensional Ga_2O_3 materials, and β - Ga_2O_3 nanowires have been obtained through physical evaporation and arc-discharge methods.⁷ β - Ga_2O_3 has also attracted recent interest as a phosphor host material for applications in thin film electroluminescent displays.^{8,9} Due to its chemical and thermal stability, β - Ga_2O_3 may emerge as a useful alternative to sulfide-based phosphors.¹⁰

It is well known that Ga_2O_3 can exist in several forms, including α , β , γ , δ , and ϵ polymorphs that all have different structure types.¹¹ Of these, the most stable form at ambient conditions is determined to be β - Ga_2O_3 .¹¹ However, other metastable varieties can be prepared and they have been characterized at ambient pressure and temperature. This is an important observation, because the different forms have dramatically different optoelectronic properties. For example, the band gap of the α - Ga_2O_3 polymorph that is isostructural with corundum (α - Al_2O_3) is 2.41 eV, much narrower than that of β - Ga_2O_3 .¹²

It is of great interest to determine the pressure-induced phase transformations among Ga_2O_3 polymorphs in order to establish the stable and metastable phase relations between different crystalline modifications, and to evaluate their production under different synthesis conditions. It is particularly important to understand the role of differential mechanical stresses that are present during thin film deposition, or in

creation of nanoparticles or nanowires, in promoting the formation of specific polymorphic forms. At present, little is known about pressure-induced phase transitions in Ga_2O_3 .

The high-pressure behavior of Al_2O_3 compounds has been studied extensively, particularly the corundum-structured α - Al_2O_3 phase, because of its importance as a mineral structure within the deep Earth and also due to the widespread use of ruby (Cr^{3+} -doped α - Al_2O_3) as a luminescent pressure gauge for *in situ* high-pressure experiments in the diamond anvil cell.¹³ Cr^{3+} -doped β - Ga_2O_3 has likewise been proposed as a pressure gauge material. The R1 luminescence line in this phase shows a pressure shift nearly three times that of ruby, indicating that it would make a more sensitive pressure sensor that is especially useful in the lower pressure range.¹⁴ *In situ* high-pressure and high-temperature measurements on α - Al_2O_3 using synchrotron x-ray diffraction in a diamond anvil cell, combined with *ab initio* theory predictions, have now been used to characterize a transition into the Rh_2O_3 -II structure occurring at $P\sim 100$ GPa and $T>\sim 1000$ K.^{15,16}

The high-pressure behavior of Ga_2O_3 has received much less attention. The various low-density Ga_2O_3 structures encountered at low pressure contain the Ga^{3+} cations in tetrahedral coordination (i.e., GaO_4 species). The thermodynamically stable β - Ga_2O_3 polymorph is isomorphous with the metastable θ - Al_2O_3 structure, which represents a key phase achieved during metastable transformations among various partially dehydrated “transitional” aluminas as they evolve towards corundum¹⁷ (Fig. 1). θ - Al_2O_3 constitutes an intermediate structure between the cubic close packing of anions achieved within the low-temperature metastable aluminas, and hexagonally close-packed α - Al_2O_3 corundum (isomorphous with α - Ga_2O_3).

In a recent study using synchrotron energy-dispersive x-ray diffraction techniques in the diamond anvil cell, it was reported that a sample of “ α - Ga_2O_3 ” transformed to a structure assigned to be tetragonal at a pressure of approximately 13.3 GPa.¹⁸ However, the x-ray diffraction pattern of the starting material most strongly resembled that of β - Ga_2O_3 , rather than the α -form, and a mixture of phases was

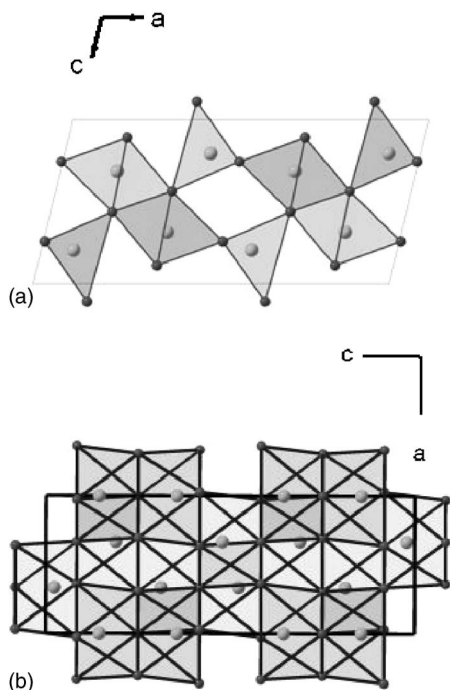


FIG. 1. (a) projection of the monoclinic structure of $\beta\text{-Ga}_2\text{O}_3$ onto the a - c plane. Note the Ga^{3+} cations that occupy both tetrahedral and octahedral interstices within the ccp lattice of O^{2-} ions. (b) a - c projection of corundum-structured $\alpha\text{-Ga}_2\text{O}_3$, containing only octahedrally coordinated Ga^{3+} ions, within an hcp O^{2-} sublattice.

present. Commercial Ga_2O_3 samples usually consist mainly of $\beta\text{-Ga}_2\text{O}_3$, along with some $\alpha\text{-Ga}_2\text{O}_3$; that phase can be removed by heat treatment.¹¹ The relative densities of β - and $\alpha\text{-Ga}_2\text{O}_3$ are 5.94 and 6.48 g cm^{-3} , respectively,¹⁹ indicating that a $\beta \rightarrow \alpha$ transformation should occur at high pressure. Nanocrystalline $\beta\text{-Ga}_2\text{O}_3$ particles embedded in a glassy matrix were also studied at high pressure using energy-dispersive x-ray diffraction.²⁰ In that work, a β -to- α phase transformation was found to be initiated at 6 GPa, but the process was not completed by 15 GPa, the highest pressure achieved in the study. However, it is known that the silica glass host matrix undergoes important structural and density changes within this pressure range,^{21,22} so that it is not yet known if the structural changes are intrinsic to the $\beta\text{-Ga}_2\text{O}_3$ material (presumably influenced by the nanocrystalline nature of the sample), or are promoted by anomalous densification among the SiO_2 matrix. These results prompted us to re-examine the high-pressure behavior occurring within phase-pure bulk samples of $\beta\text{-Ga}_2\text{O}_3$, using Raman spectroscopy and high-resolution synchrotron x-ray diffraction (angle dispersive) techniques. Our study was also motivated by the recent high-pressure, high-temperature synthesis of spinel-structured gallium oxynitride, from chemical precursors or $\text{GaN} + \text{Ga}_2\text{O}_3$, which necessitated a better understanding of the end-member oxide phase.^{23,24}

II. EXPERIMENTAL AND COMPUTATIONAL PROCEDURES

Commercially available Ga_2O_3 powder (Aldrich 99.995% chemical purity) consists of a mixture of β - and α -phases

with an approximate ratio 70/30 according to x-ray diffraction data. This mixture was annealed at 800 °C for 12 h to convert it to a pure sample of the $\beta\text{-Ga}_2\text{O}_3$ form for the present study. The crystallites were found to be on a scale of several micrometers in dimension, by direct optical inspection.

High-pressure Raman scattering experiments were carried out using a diamond anvil cell of cylindrical design with low-fluorescence diamonds having a culet size of 200 μm . The powdered sample was loaded into a 90 μm hole drilled in a Re gasket. The pressure-transmitting medium was Ar cryogenically loaded as a fluid into the cell, and used as a nearly hydrostatic medium during pressurization experiments. Several ruby chips were distributed throughout the sample chamber, and the pressures were determined using the ruby fluorescence method.¹³ Raman spectra were obtained using a home-built high-throughput optical system based on Kaiser optical filters and an Acton 300i spectrograph with sensitive CCD detection.²⁵ Spectra were excited using 514.5 nm radiation from an air-cooled Ar^+ laser. The beam was focused on to the sample using a Mitutoyo 50 \times objective, with beam diameter $\sim 2 \mu\text{m}$ at the sample. The scattered light was collected in backscattering geometry using the same lens.

Synchrotron radiation measurements were performed at beamline 9.1 at the Synchrotron Radiation Source (SRS, Daresbury, United Kingdom) and also at the European Synchrotron Radiation Facility (ESRF; Swiss-Norwegian Beamlines, BM1A) via angle-dispersive diffraction techniques using monochromatic radiation ($\lambda = 0.465 \text{ \AA}$ at SRS and $\lambda = 0.700 \text{ \AA}$ at ESRF). Diffraction patterns were collected using image plate detection. The sample-to-detector distance and the image plate inclination angles were calibrated using a Si standard. The two-dimensional diffraction images were analyzed using the FIT2D software, yielding one-dimensional intensity versus diffraction angle 2θ patterns.²⁶ Samples for the synchrotron x-ray studies were loaded using various pressure-transmitting media (4:1 ethanol-methanol mixtures, silicone oil, nitrogen) that all yield reasonably hydrostatic pressurization environments over the pressure range investigated.²⁷ The results were found to be identical in each case. The pressures were determined using the ruby fluorescence method.¹³

During the course of the experimental study, we began a parallel theoretical investigation of the structures, relative energetics, and properties of Ga_2O_3 phases.²⁸ Here we report some of the preliminary results relevant to the lattice dynamics of α - and $\beta\text{-Ga}_2\text{O}_3$ phases, which were carried out in order to interpret the experimental spectra. Our calculations are based on the first-principles density functional theory within the local density approximation (LDA). The calculations were carried out with the VASP codes,²⁹ using plane-wave basis sets and ultrasoft pseudopotentials (USPP).³⁰ We have applied calculations of this type to obtain lattice dynamical information in a wide range of systems, including main group oxides³¹ and nitrides.³² In this study, both valence ($4s4p$) and semi-core ($3d$) electrons in Ga atoms were treated explicitly, while the core electrons were approximated with the USPP. The energy cutoff of the plane-wave basis was chosen as 396 eV. The Brillouin zone integration

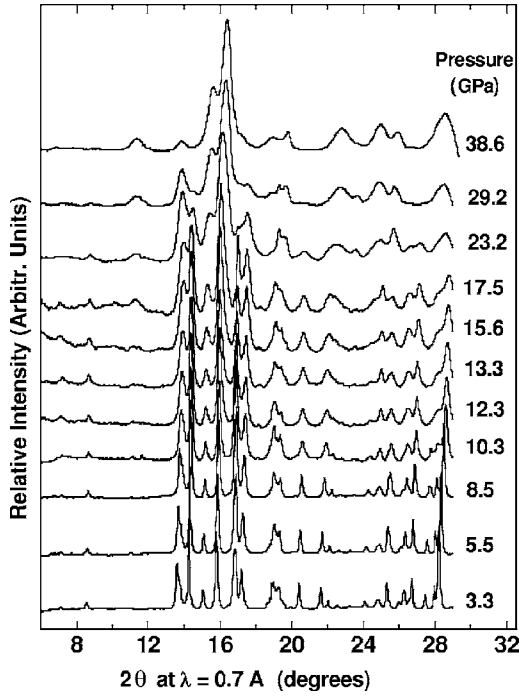


FIG. 2. X-ray diffraction patterns obtained during compression of the β - Ga_2O_3 phase at ambient temperature.

of total energy of the unit cells was carried out using $6 \times 6 \times 6$ grids for both phases.

The phonon dynamical matrices $D_{ij}(\vec{k})$ were constructed at the Brillouin zone center (Γ -point: $\vec{k}=0$) using a (real-space) force constant matrix $\phi_{ij}(\vec{r})$ by calculating forces on each atom as it is slightly displaced from its equilibrium position (e.g., by 0.015 Å). Further approximations were adopted to calculate the $D_{ij}(\vec{k})$ matrix at a general \vec{k} -point. In the case of α - Ga_2O_3 , we first obtained the real space $\phi_{ij}(\vec{r})$ matrix using a 120-atom supercell model. Because of the large size of the supercell model, and the fact that the material is insulating (wide-gap semiconducting), we can safely neglect interatomic interactions between atoms separated by $>50\%$ of the supercell lattice constants, and thus obtain $D_{ij}(\vec{k})$ by Fourier transformation of the real-space matrix elements $\phi_{ij}(\vec{r})$. Further details of our calculation methods of lattice dynamics have been described previously.^{33,34}

III. EXPERIMENTAL RESULTS

A. X-ray diffraction

During *in situ* synchrotron x-ray diffraction experiments on β - Ga_2O_3 , the pressure was increased in steps of 2–3 GPa. Selected diffraction patterns are shown in Fig. 2. No changes in the diffraction pattern were observed below 20 GPa, indicating that the previous suggestion of a phase transition occurring in this range is incorrect.¹⁸ Some broadening in the diffraction lines occurs at pressures above 10–12 GPa, independent of the pressurization medium used (Fig. 2). LeBail refinements were carried out at various pressures using the FULLPROF software³⁵ to obtain cell parameters for the

β - Ga_2O_3 structure. The evolution of the monoclinic cell parameters with pressure is presented in Fig. 3, and the linear compressibilities are summarized in Table I. The compressibility values along the b and c axes are comparable with those obtained previously for nanocrystalline samples embedded in SiO_2 ,²⁰ however, the a -axis compression is twice as large for the bulk sample compared with the nanoparticles (Table I). Between 0 and 20 GPa, we observed a decrease of only 0.5° in the monoclinic angle, whereas in the nanocrystalline sample, this parameter was found to decrease by 2° over the same pressure range.

The V/V_0 relations as a function of pressure are shown in Fig. 4(a). The data were fitted using a third-order Birch-Murnaghan equation of state, using refined values of $K_0 = 202(7)$ GPa and $K'_0 = 2.4(6)$. The K_0 and K'_0 values were obtained using a reduced variable F - f plot [Fig. 4(b)], representing the data in terms of the Eulerian strain parameter (f) and the normalized pressure (F), defined by

$$f = \frac{1}{2} \left[\left(\frac{V}{V_0} \right)^{-2/3} - 1 \right],$$

$$F = P[3f(1+2f)^{2.5}]^{-1}.$$

This formalism yields the second-order finite-strain equation

$$F = K_0[1 - 1.5(4 - K'_0)f].$$

K_0 and K'_0 were then obtained as the intercept as $F \rightarrow 0$ and the slope of the $F(f)$ plot, respectively [Fig. 4(b)].

A large change in the diffraction patterns was observed to occur beginning at pressures above 20 GPa, with the appearance of additional peaks indicating occurrence of a phase transition. Over the pressure range 20–29 GPa, weak reflections from the β -phase could still be detected in the diffraction patterns, indicating that the transformation was of the first order and proceeded slowly at ambient temperature. By 39 GPa, only peaks from the high-pressure phase remained (Fig. 2). The new diffraction pattern could be indexed within the $R\bar{3}c$ space group expected for the α - Ga_2O_3 structure that is isostructural with corundum (α - Al_2O_3) (Fig. 5). The lattice parameters refined within this space group for the new phase at 38.6 GPa were $a = 4.920(5)$ Å and $c = 12.99(1)$ Å. The diffraction peaks of the high-density phase were significantly broadened compared with those for β - Ga_2O_3 at lower pressure, indicating that structural disorder was present. This is in agreement with the Raman data presented below. A bulk modulus $K_0 \sim 250$ GPa for α - Ga_2O_3 was estimated from the patterns obtained at high pressure. This value is comparable with that measured for α - Al_2O_3 ($K_0 = 253$ GPa).³⁶ Upon “rapid” decompression, i.e., from 25 GPa to ambient pressure in 5 min, the high-density phase could be recovered to ambient pressure. The full width at half-maximum measured for the diffraction peaks of the recovered sample at ambient pressure is 0.44° on average, whereas that for β - Ga_2O_3 before compression is 0.15° on average. This broadening denotes the presence of structural disorder in the decompressed sample.

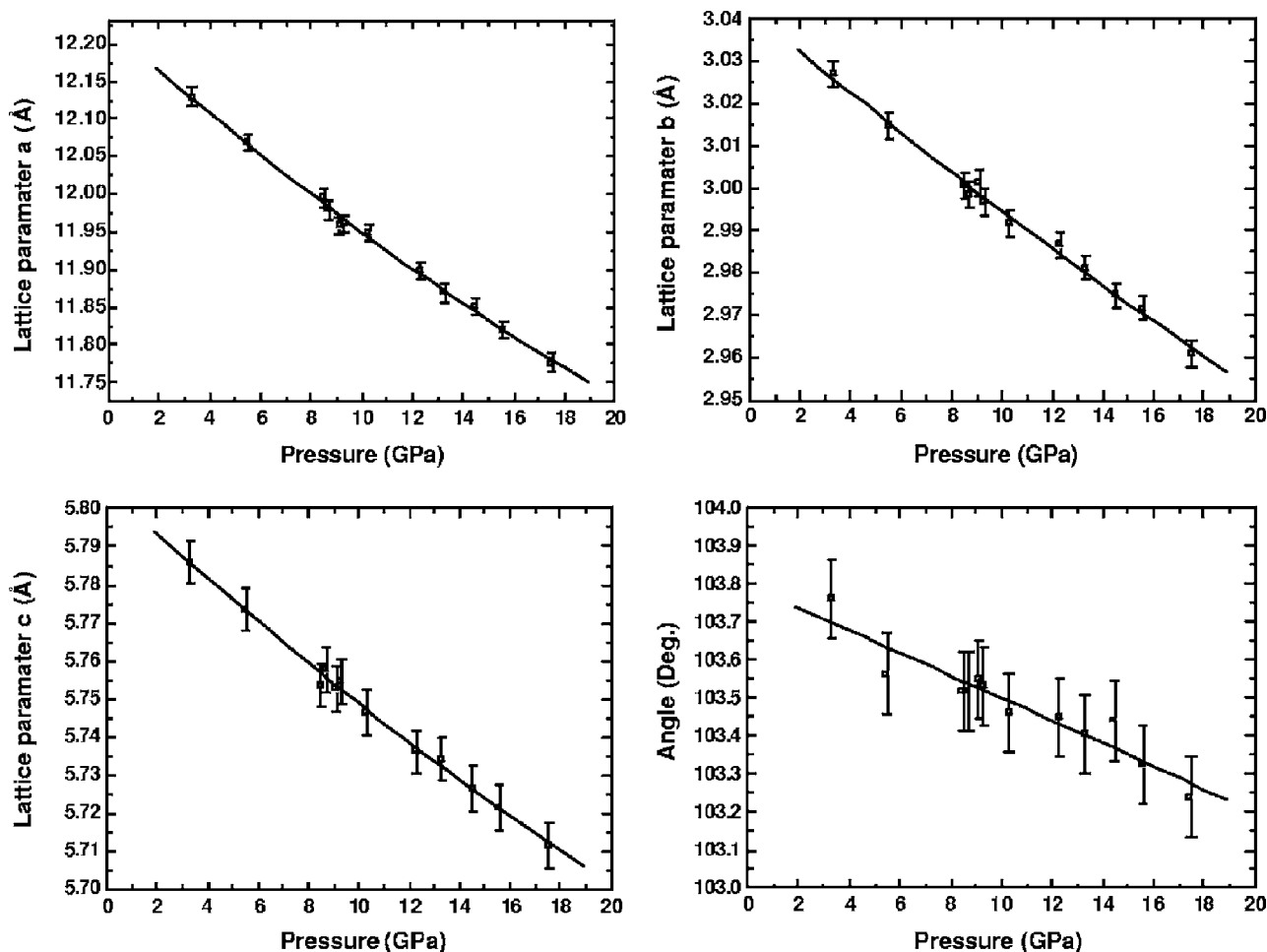


FIG. 3. Evolution of the cell parameters of β -Ga₂O₃ with pressure. The solid lines are drawn as a guide to the eye.

B. Raman spectroscopy

Fifteen Raman-active modes are expected for the β -Ga₂O₃ structure (point symmetry C_{2h}^3) from symmetry analysis:

$$\Gamma_{\text{raman}} = 10 A_g + 5 B_g.$$

An unpolarized Raman spectrum of β -Ga₂O₃ was recorded from powdered material obtained by annealing a commercial sample (Fig. 6). The observed frequencies and their mode Grüneisen parameters are reported in Table II. The spectrum

is in good agreement with previously published data.³⁷ We also used our LDA calculations to predict the Raman-active modes in order to assign the mode symmetries. In general, the calculated frequencies agree well with the observed values, to within 0.1%–6%, which is typical for LDA calculations (Table II). The B_g mode predicted at 356 cm⁻¹ was likely unresolved from the A_g mode at 346 cm⁻¹ in our study (Fig. 6); however, a weak peak at this frequency was recorded by Dohy *et al.*³⁸ The band observed at 474 cm⁻¹ also likely contains contributions from the calculated A_g and B_g

TABLE I. Comparison of the mechanical properties of the β -Ga₂O₃ polymorph and pressure of transition obtained in the present work with those reported in Ref. 20.

	Bulk material (this study)	Nanocrystalline material (Ref. 20)
Transition pressure	25 GPa	6 GPa
β_a	$1.99(9) \times 10^{-3} \text{ GPa}^{-1}$	$8.2 \times 10^{-4} \text{ GPa}^{-1}$
β_b	$1.45(2) \times 10^{-3} \text{ GPa}^{-1}$	$1.97 \times 10^{-3} \text{ GPa}^{-1}$
β_c	$8.8(4) \times 10^{-4} \text{ GPa}^{-1}$	$8.8 \times 10^{-4} \text{ GPa}^{-1}$
K_0	202(7) GPa	191(5) GPa
K'_0	2.4(6)	8.3(9)

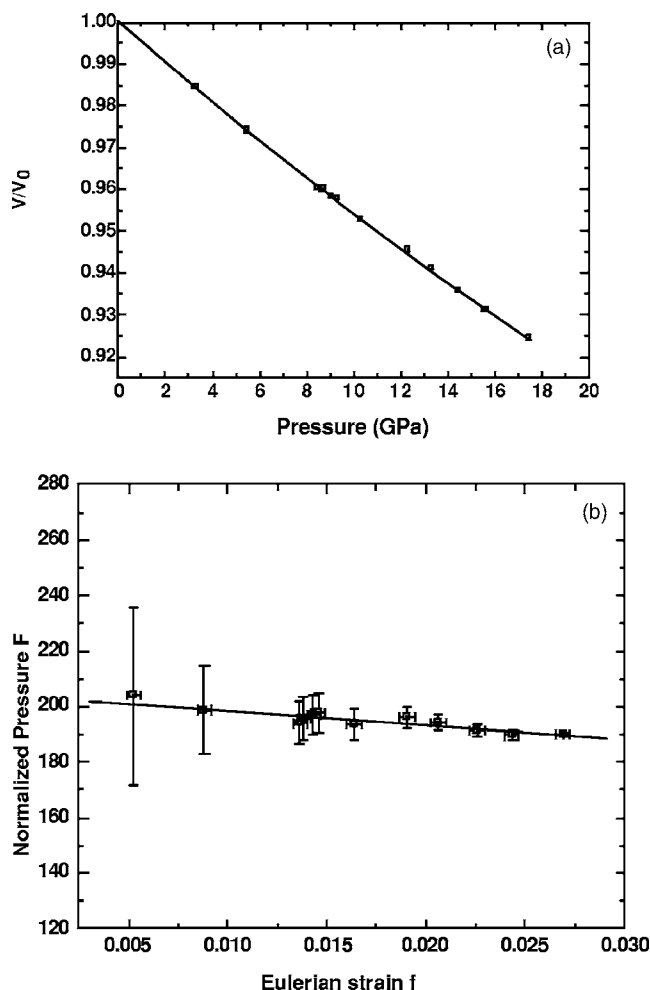


FIG. 4. (a) Plot of measured V/V_0 for β - Ga_2O_3 as a function of pressure (points) along with a third-order Birch-Murnaghan equation of state fitted to the data with $K_0=202(7)$ GPa and $K'_0=2.4(6)$. The K_0 and K'_0 values were obtained from a reduced variable (F - f) plot. (b) Plot of the normalized pressure (F) as a function of the Eulerian strain variable (f) for β - Ga_2O_3 .

modes at 467 and 474 cm^{-1} . Surprisingly, we found no experimental evidence for the predicted A_g mode at 600 cm^{-1} . We have no explanation for that observation.

The x-ray diffraction results indicate that the high-density phase present above 20 GPa following the pressure-induced transition likely corresponds to α - Ga_2O_3 , and that the material likely exhibits structural disorder. In order to help interpret the results of the Raman data obtained at high pressure, we recorded an ambient pressure spectrum for a well-crystallized sample of α - Ga_2O_3 (Fig. 7). This material was obtained from a gel formed by adding NH_3 to aqueous nitrate solution.¹¹ It was prepared at the University of Kent (Canterbury) by P. Allen,³⁹ and kindly supplied by Prof. A.V. Chadwick. Symmetry analysis indicates that seven Raman active modes are expected for the corundum structure:

$$\Gamma_{\text{raman}} = 2 A_{1g} + 5 E_g.$$

We observed all seven modes as sharp peaks in the Raman spectrum. The observed frequencies agree to within

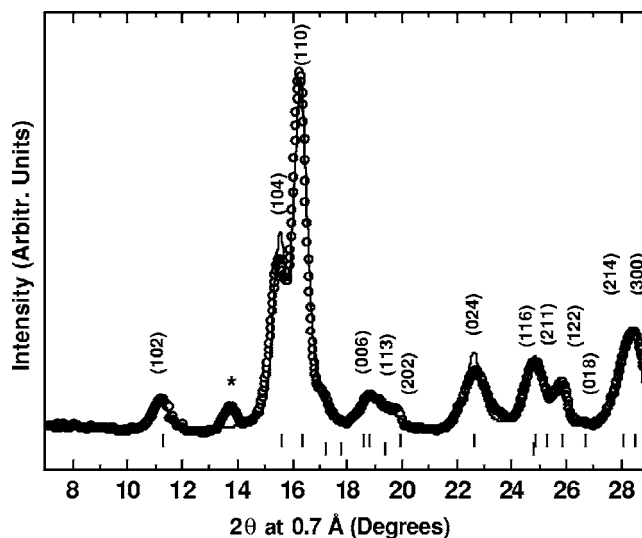


FIG. 5. An example of a profile-refined x-ray diffraction data set collected at 38.6 GPa. The open symbols represent experimental data; the solid curve running through the data corresponds to the calculated pattern. The tick marks indicate the positions of calculated Bragg reflections of α - Ga_2O_3 (indexed on the pattern), and also for Re used as the gasket material. Asterisks show additional peaks that can be assigned to a trace amount of β - Ga_2O_3 , remaining in the sample even at this high pressure.

0.7%–5.5% with the theoretically predicted values (Table III).

During the compression study, the Raman spectrum contained only features assigned to β - Ga_2O_3 up to P of 20–22 GPa (Fig. 8). The spectrum of β - Ga_2O_3 became slightly modified in the 16–20 GPa range, in that a broad band appeared near 260 cm^{-1} , and this feature strengthened with increasing pressure (Fig. 8). This band may indicate some disordering occurring within the β - Ga_2O_3 structure premonitory to the structural phase transformation. At 25 GPa, the strongest Raman peak of the β - Ga_2O_3 phase near 200 cm^{-1} is

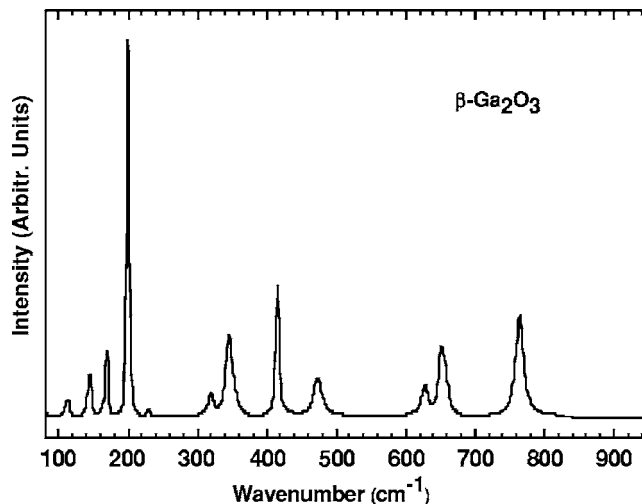
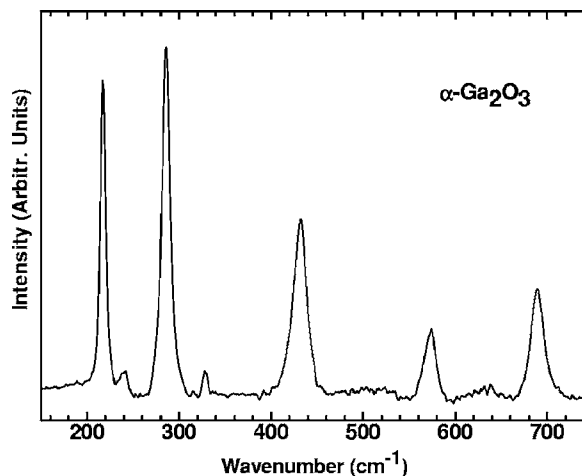


FIG. 6. Unpolarized Raman spectrum of β - Ga_2O_3 obtained after annealing a commercial sample. A weak peak at 222 cm^{-1} is due to a trace of α - Ga_2O_3 remaining after the heat treatment.

TABLE II. Experimental and calculated zone-center Raman peak positions and Grüneisen parameter for the β -Ga₂O₃ phase.

Mode symmetry	Frequency (calculated)	Frequency (measured)	Grüneisen ratio (calculated)	Grüneisen ratio (measured)
A_g	104	110.2	1.39	
B_g	113	113.6	-0.7	
B_g	149	144.7	1.53	1.97(8)
A_g	165	169.2	1.00	0.35(3)
A_g	205	200.4	1.30	0.98(2)
A_g	317	318.6	1.13	0.95(1)
A_g	346	346.4	1.83	1.52(1)
B_g	356		1.47	—
A_g	418	415.7	0.58	0.78(4)
A_g	467		1.26	—
B_g	474	473.5	1.14	1.27(9)
A_g	600		1.70	—
B_g	626	628.7	0.8	1.54(3)
A_g	637	652.5	1.39	1.39(2)
A_g	732	763.9	1.23	1.11(1)

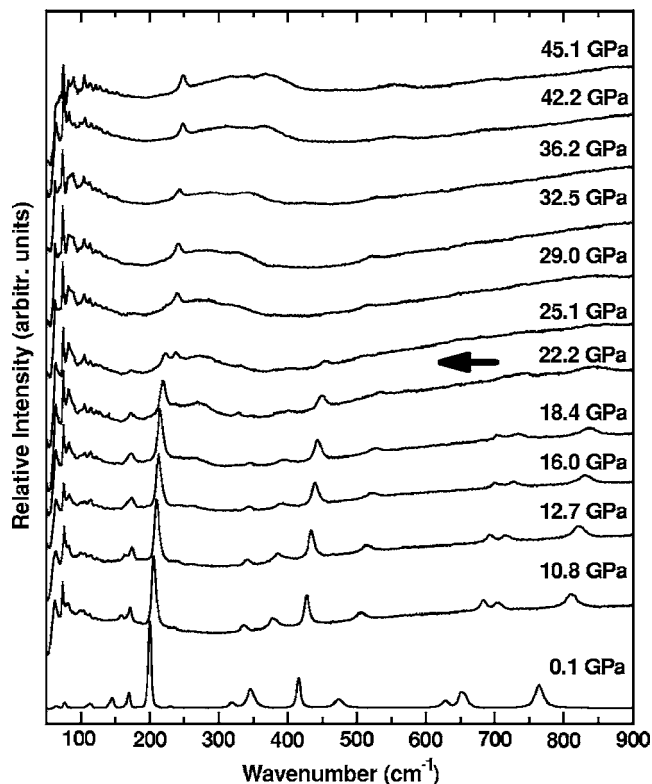
only just visible in the spectrum, and it coexists with a sharp peak near 240 cm⁻¹ that could correspond to the strongest Raman mode of the α -Ga₂O₃ structure observed at ambient pressure. That peak remains to the highest pressures investigated in this study. However, instead of the remaining sharp peaks expected for the α -Ga₂O₃ phase, we observed a series of broad bands occurring up to ~ 700 cm⁻¹. Although the x-ray results demonstrate that a pressure-induced transition to the α -polymorph occurs within this pressure range, the broad diffraction peaks also indicate that structural disorder is present. That could result in destruction of the local translational symmetry rules for observation of zone-center Raman active modes (i.e., the $\mathbf{k}=\mathbf{0}$ criterion), and a broadened

FIG. 7. Unpolarized Raman spectrum of α -Ga₂O₃ obtained from the synthesis described in Ref. 11. The sample was obtained from Prof. A.V. Chadwick, University of Kent at Canterbury.TABLE III. Experimental and calculated zone-center Raman peak positions for the α -Ga₂O₃ phase.

Mode symmetry	Frequency (calculated)	Frequency (measured)
A_{1g}	215	217.4
E_g	239	240.8
E_g	281	286.1
E_g	344	328.7
E_g	410	432.2
A_{1g}	551	573
E_g	680	688.1

vibrational density of states function [VDOS, or $g(\omega)$] would be observed.

$g(\omega)$ for α -Al₂O₃ has previously been calculated theoretically using density functional methods.⁴⁰ These workers also calculated $g(\omega)$ for θ -Al₂O₃, that is isomorphic with β -Ga₂O₃. In our theoretical work, we obtained the VDOS for α -Ga₂O₃ (Fig. 9). However, we discovered that β -Ga₂O₃ within the monoclinic $C2/m$ structure exhibited dynamical instabilities away from the Brillouin zone center, so that we could not obtain a reliable $g(\omega)$ function. These detailed results and their implications will be reported elsewhere.²⁸ The $g(\omega)$ for the corresponding θ -Al₂O₃ structure does not correspond at all with the observed broad bands in our spectra at high pressure. The VDOS for α -Ga₂O₃ exhibits a broad band

FIG. 8. Raman spectra of Ga₂O₃ obtained during “slow” compression.

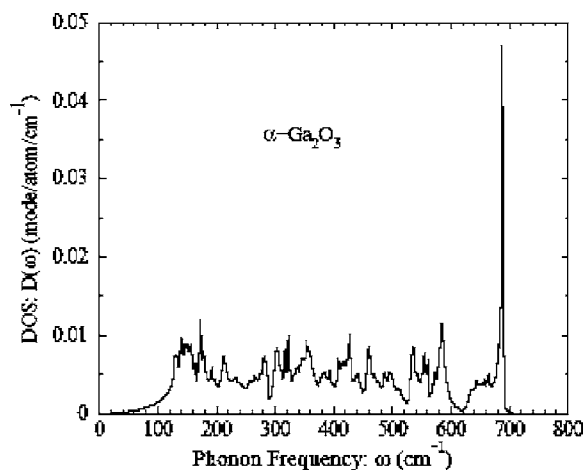


FIG. 9. Calculated VDOS for α -Ga₂O₃, using *ab initio* (LDA) theoretical methods.

of frequencies between 100 and 600 cm⁻¹, which generally covers the range observed experimentally. There is one peak in $g(\omega)$ at ~ 220 cm⁻¹, which could correspond to the sharp feature observed in the Raman spectra (Fig. 7). However, a sharp band-edge feature is also predicted to occur at 700 cm⁻¹, which is not observed in the experimental data at high pressure (Fig. 8). The x-ray diffraction data suggest that the high-pressure form of Ga₂O₃ corresponds to the α - polymorph, which may contain some structural disorder. The Raman data generally correspond to a VDOS function enabled by structural disorder; however, the observed spectra compared with the theoretical results indicate that the underlying structure of the high-density phase may be subtly different to that of α -Ga₂O₃. In Fig. 10, we show the spectral evolution observed during a “rapid” compression, in which the sample was squeezed from 1.7 to 18.3 GPa in few minutes and left to equilibrate for 12 h. The spectrum at 18.3 GPa shows the same broad feature as observed in the low-rate compression run.

When samples were decompressed “slowly” (i.e., using small pressure steps, interrupted by 15–30 minute periods at

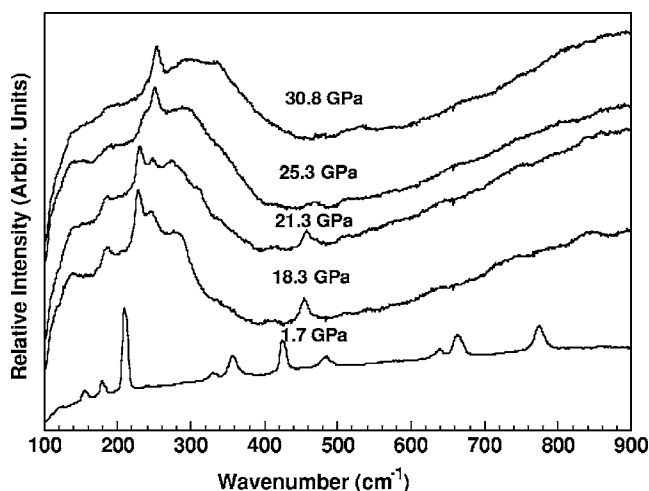


FIG. 10. Raman spectra of Ga₂O₃ obtained during “rapid” compression.

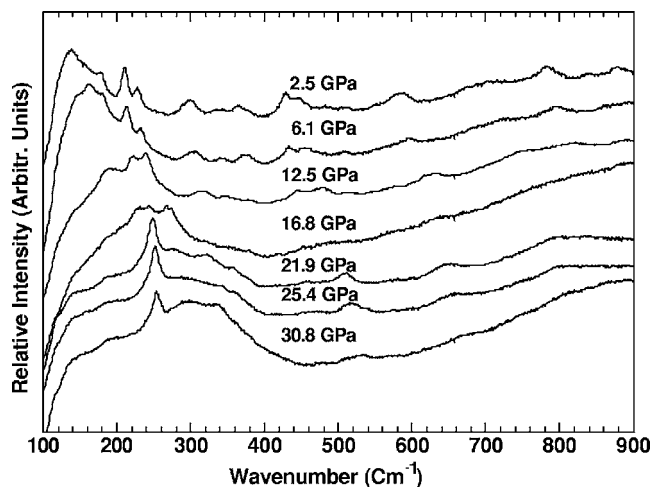


FIG. 11. Raman spectra of Ga₂O₃ during “slow” decompression.

ambient T at each pressure during which Raman spectra were obtained), the large band centered around 320 cm⁻¹ decreased in intensity between 30.8 and 21.9 GPa. A sluggish transformation clearly occurs between 21.9 and 12.5 GPa, associated with dramatic changes in the Raman spectrum. The well-resolved peak at 240 cm⁻¹ disappears and new peaks are observed (e.g., at 280 and 420 cm⁻¹). The spectrum obtained at 2.5 GPa could be interpreted as a mixture of α -Ga₂O₃ and β -Ga₂O₃ indicating a back-transformation to the β -Ga₂O₃ phase occurs (Fig. 11). However, the peaks recorded for the recovered sample are broadened compared with the starting material. During a “rapid” decompression with a pressure jump directly from 20 GPa down to ambient pressure (Fig. 12), the back-transformation was not observed, and the high-density phase with a diffraction pattern that was indexed as the α -Ga₂O₃ corundum structure could be quenched to ambient pressure. Peaks that appear in the Raman spectrum are comparable with those measured for well-crystallized α -Ga₂O₃; however, additional broad features are also present.

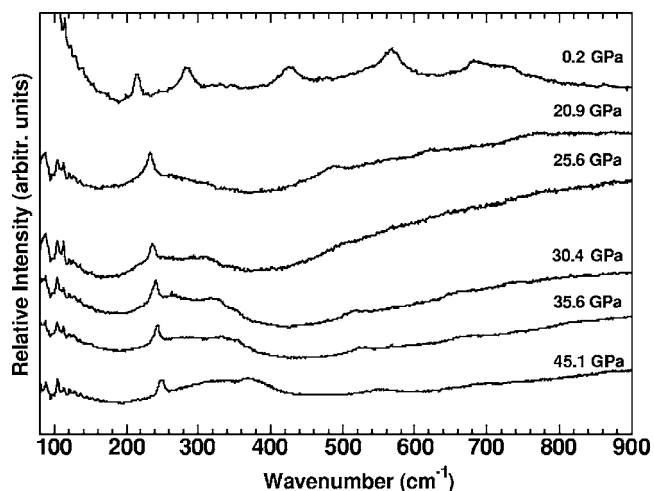


FIG. 12. Raman spectra of Ga₂O₃ during “rapid” decompression.

IV. DISCUSSION

The monoclinic β -Ga₂O₃ structure is the stable polymorph at ambient pressure and temperature.²⁵ In this phase, the O²⁻ anions form a slightly distorted fcc lattice and cations occupy tetrahedral and octahedral interstices (Fig. 1). This structure is quite different from that of the α -Ga₂O₃ phase (corundum structure), which is based on a distorted hcp O²⁻ sublattice with 2/3 of the octahedral interstices occupied by Ga³⁺ ions (Fig. 1). The $\beta \rightarrow \alpha$ transition is expected to result from increasing the pressure, from the observed density relationships between the two phases. The transformation involves a change in the O²⁻ packing from cubic to hexagonal, accompanied by a shift in Ga³⁺ ions between tetrahedral and octahedral sites. The reconstructive nature of the transition indicates that it is thermodynamically of the first order, and it might be expected to involve a large activation energy, which gives rise to slow transformation kinetics at low temperature. In addition, the high-density structure has significant possibilities for disorder among the Ga³⁺ positions on octahedral sites within the hcp O²⁻ sublattice, which might not be readily detected by x-ray diffraction.¹⁵

The x-ray diffraction and Raman scattering results on β -Ga₂O₃ clearly indicate that a pressure-induced phase transformation occurs within the $P=20$ – 22 GPa range, and perhaps as low as $P=18.5$ GPa. Analysis of the x-ray diffraction data suggest that the high-density phase corresponds to corundum-structured α -Ga₂O₃. However, broadening observed both in the x-ray diffraction peaks and in the Raman spectra indicate that the material is structurally disordered. We are presently examining in more detail the mechanisms of solid-state transformations between β -Ga₂O₃ with an fcc O²⁻ sublattice and various hcp phases related to “ α -Ga₂O₃”.⁴¹

The high-pressure behavior of bulk Ga₂O₃ differs considerably from that of nanocrystalline Ga₂O₃ particles embed-

ded in a silica matrix. The onset of the phase transition pressure is found to be much lower in the nanocrystalline sample (~ 6 GPa, rather than 18–22 GPa in the bulk material) (Table I). However, it is already known that the thermodynamics of phase transition within nanocrystalline samples are considerably altered compared with those for bulk materials. In addition, the $\beta \rightarrow \alpha$ phase transition observed for nc-Ga₂O₃ could be significantly affected by the host silica glass matrix, which exhibits an unusually large densification in this pressure range.^{21,22}

V. CONCLUSION

The high-pressure behavior of β -Ga₂O₃ was investigated using high-resolution angle-dispersive synchrotron x-ray diffraction and Raman scattering. A phase transformation was observed to occur at above $P \sim 20$ GPa, resulting in a high-density Ga₂O₃ polymorph that is structurally related to α -Ga₂O₃ (corundum structure). However, the Raman spectra and broadened x-ray diffraction lines indicate that the phase is structurally disordered. The disorder could occur due to occupancy of the Ga³⁺ cations among the octahedral sites within the hexagonally close-packed layers of the O²⁻ sublattice.

ACKNOWLEDGMENTS

This study was supported by a UK EPSRC grant to P.F.M., who also receives support from the Wolfson-Royal Society. The theoretical work at Auburn University was supported by a U.S. DOE grant to J.D. (DE-FG02-03ER46060). We thank A. V. Chadwick (Canterbury) for providing a sample of α -Ga₂O₃. A. Lennie and M. Roberts from the UK Synchrotron Radiation Source are thanked for their experimental assistance. Experimental assistance from the staff of the Swiss-Norwegian Beam Lines, especially from V. Dmitriev, at ESRF is gratefully acknowledged.

*Author to whom correspondence should be addressed. Email address: p.f.mcmillan@ucl.ac.uk

¹G. Schmitz, P. Gassmann, and R. Franchy, *J. Appl. Phys.* **83**, 2533 (1998).

²M. Fleischer and H. Meixner, *J. Mater. Sci. Lett.* **11**, 1728 (1992).

³M. Passlack *et al.*, *J. Appl. Phys.* **77**, 686 (1995).

⁴M. Fleischer and H. Meixner, *Sens. Actuators B* **4**, 437 (1991).

⁵E. Aubay and D. Gourier, *Phys. Rev. B* **47**, 15023 (1993).

⁶M. Passlack *et al.*, *Appl. Phys. Lett.* **64**, 2715 (1994).

⁷Y. C. Choi, W. S. Kim, Y. S. Park, S. M. Lee, D. J. Bae, Y. H. Lee, G. Park, W. B. Choi, N. S. Lee, and J. M. Kun, *Adv. Mater. (Weinheim, Ger.)* **12**, 746 (2000).

⁸T. Miyata, T. Nakatani, and T. Minami, *J. Lumin.* **87-89**, 1183 (2000).

⁹T. Xiao, A. H. Kitai, G. Liu, A. Nakua, and J. Barbier, *Appl. Phys. Lett.* **72**, 3356 (1998).

¹⁰J. Hao and M. Cocivera, *J. Phys. D* **35**, 433 (2002).

¹¹R. Roy, V. G. Hill, and E. F. Osborn, *J. Am. Chem. Soc.* **74**, 719

(1952).

¹²H. G. Kim and W. T. Kim, *J. Appl. Phys.* **62**, 2000 (1987).

¹³H. K. Mao, P. M. Bell, J. W. Shaner, and D. J. Steinberg, *J. Appl. Phys.* **49**, 3276 (1978).

¹⁴T. P. Beales, C. H. L. Goodman, and K. Scarrot, *Solid State Commun.* **73**, 1 (1990).

¹⁵N. Funamori and R. Jeanloz, *Science* **278**, 1109 (1997).

¹⁶K. T. Thomson, R. M. Wentzcovitch, and M. S. T. Bukowinski, *Science* **274**, 1880 (1996).

¹⁷R.-S. Zhou and R. L. Snyder, *Acta Crystallogr., Sect. B: Struct. Sci.* **47**, 617 (1991).

¹⁸B. Tu *et al.*, *J. Phys.: Condens. Matter* **14**, 10627 (2002).

¹⁹J. P. Remeika and M. Marezio, *Appl. Phys. Lett.* **8**, 87 (1966).

²⁰K. E. Lipinska-Kalita, B. Chen, M. B. Kruger, Y. Ohki, J. Murowchick, and E. P. Gogol, *Phys. Rev. B* **68**, 035209 (2003).

²¹M. Grimsditch, *Phys. Rev. Lett.* **52**, 2379 (1984).

²²C. Meade, R. J. Hemley, and H.-K. Mao, *Phys. Rev. Lett.* **69**, 1387 (1992).

- ²³E. Soignard, D. Machon, P. F. McMillan, J. Dong, B. Xu, and K. Leinenweber, *Chem. Mater.* **17**, 5465 (2005).
- ²⁴J. E. Lowther, T. Wagner, I. Kinski, and R. Riedel, *J. Alloys Compd.* **376**, 1 (2004).
- ²⁵E. Soignard and P. F. McMillan, *Chem. Mater.* **16**, 3533 (2004).
- ²⁶A. P. Hammersley, S. O. Svensson, M. Hanfland, A. N. Fitch, and D. Hausermann, *High Press. Res.* **14**, 235 (1996).
- ²⁷A. Jayaraman, *Rev. Mod. Phys.* **55**, 65 (1983).
- ²⁸J. Dong *et al.* (unpublished).
- ²⁹G. Kresse and J. Hafner, *Phys. Rev. B* **47**, R558 (1993); G. Kresse and J. Furthmuller, *Comput. Mater. Sci.* **6**, 15 (1996).
- ³⁰D. Vanderbilt, *Phys. Rev. B* **41**, R7892 (1990); G. Kresse and J. Hafner, *J. Phys.: Condens. Matter* **6**, 8245 (1994).
- ³¹J. Dong, J. K. Tomfohr, O. F. Sankey, K. Leinenweber, M. Somayazulu, and P. F. McMillan, *Phys. Rev. B* **62**, 14685 (2000).
- ³²J. Dong, J. Deslippe, O. F. Sankey, E. Soignard, and P. F. McMillan, *Phys. Rev. B* **67**, 094104 (2003); J. Dong, A. A. Kinkhabwala, and P. F. McMillan, *Phys. Status Solidi B* **241**, 2319 (2004).
- ³³J. Dong and O. F. Sankey, *J. Phys.: Condens. Matter* **11**, 6129 (1999).
- ³⁴J. Dong and A. B. Chen, in *SiC Power Materials Devices and Applications*, edited by Z. C. Feng (Springer, Berlin, 2005).
- ³⁵J. Rodriguez-Carjaval, *Physica B* **192**, 55 (1993).
- ³⁶J. H. Gieske and G. R. Barsch, *Phys. Status Solidi* **29**, 121 (1968).
- ³⁷J. Li, X. Chen, Z. Qiao, M. He, and H. Li, *J. Phys.: Condens. Matter* **13**, L937 (2001).
- ³⁸D. Dohy, G. Lucazeau, and A. Revcolevschi, *J. Solid State Chem.* **45**, 180 (1982).
- ³⁹P. Allen, graduate thesis, University of Kent, 2005.
- ⁴⁰Z. Lodziana and K. Parlinski, *Phys. Rev. B* **67**, 174106 (2003).
- ⁴¹M. Wilson *et al.* (unpublished).